

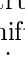



ADVANCED MORPHOLOGY OF VIPERS GALAXIES

O. Gugnin¹, A. Tugay¹, N. Pulatova^{2,3}, L. Zadorozhna^{1,4}

¹*Taras Shevchenko National University of Kyiv, 4, Glushkova ave., Kyiv, UA-03127, Ukraine,*

²*Main Astronomical Observatory of National Academy of Science of Ukraine,
27, Akademika Zabolotnoho St., Kyiv, UA-03143, Ukraine,*

³*Max-Planck-Institut für Astronomie, Königstuhl 17, D-69117 Heidelberg, Germany,*

⁴*Faculty of Physics, Astronomy and Applied Computer Science,
Jagiellonian University, 30-348 Kraków, Poland*

(Received 10 December 2021; in final form 22 February 2022; accepted 05 April 2022; published online 14 June 2022)

We calculated morphological parameters for a test sample of 4659 galaxies from VIPERS (spectroscopic galaxy survey performed on VIMOS spectroscope at VLT). These parameters include Gini, M_{20} , Concentration, Asymmetry, and Smoothness, also known as CAS parameters. The results correlate with the distribution of these parameters for other simulated and observed samples. We also studied the dependence of these parameters with the Sersic power index of the radial distribution of the surface brightness of the galaxy image. Our aim was to find a clear division of VIPERS galaxies into elliptical and spiral. This is necessary for testing the method of the Sersic index (ns) calculation in the statmorph program. To find such bimodality, we use B–V color index from VIPERS database.

To perform the error analysis of morphological parameters, we simulated galaxy images with a random background of different magnitudes and estimated the errors as the dispersion of the parameters. We also found asymptotic values of errors of morphological parameters by increasing the numbers of mock images.

To analyse the possible variation of each morphological parameter during the convolution of close galactic images, we have simulated them to research. As a result of this investigation, we have analysed the dependence of every morphological parameter from CAS and Gini- M_{20} statistics, from the distance between galactic centers.

The differences between our results for VIPERS and Gini- M_{20} distribution for PanStarrs galaxies at $z < 0.5$ could be explained by cosmological evolution of galaxies. We found out that in modern Universe there are many more elliptical galaxies than at $z > 0.5$ which corresponds to VIPERS sample. Also we concluded that galaxy mergers were more frequent in the early Universe.

Key words: Galaxies: photometry, cosmology: large-scale structure of Universe.

DOI: <https://doi.org/10.30970/jps.26.2901>

I. INTRODUCTION

VIPERS¹ is a major galaxy survey [1] for LSS (Large Scale Structure) study [2]. It contains 91507 galaxies at redshift $0.5 < z < 1.2$, covering 24 deg^2 on the sky. Their positions are important cosmology information that was used for recovering 3D filament structure in the observed volume [3]. But in addition to the positions, it is also important to study the images of galaxies for non-uniformity in the distribution of brightness. In the first approximation, galaxy images can be considered as ellipses with the radial distribution of surface brightness given by Sersic profile [4, 5]. But there are more detailed parameters to describe the images beyond Sersic profile. Some of the best sets of advanced morphology parameters are Gini [6] and M_{20} statistics [7], Concentration [8, 9], Asymmetry [10–12], and Smoothness [9]. These parameters can be calculated by the statmorph program that was written by Rodriguez-Gomez in Python [13]. The main task of the current investigation was to use the statmorph code to calculate above parameters for VIPERS galaxies. It is a very important task because these parameters can be used

for two cosmological studies. The first one is the research into galactic merging history during the evolution of the Universe [14]. The second one is the analysis of the environmental influence on the galactic morphology [15, 16], which means that environment should have influence on the galaxy formation. The distribution of galactic parameters could be used to analyse the result of the galaxy formation.

Calculation of morphological parameters of galaxies is very important for studying the extragalactic Universe, because, as it was mentioned above, the process of galaxies merging is bound with its morphological features. For these galaxies, their appearance and any physical parameters are highly dependent on the morphological types [16], masses [16], redshifts [4, 14], environments [15, 16], and the previous star formation and merging histories of the individual galaxies [4, 14, 15].

It is very useful to study the influence of the environment on galaxy formation and merging too, because, as it is said in [16], there is a correlation between the environment and the galactic type, which can be obtained from the knowledge of morphological parameters, e.g. early-type galaxies are preferentially found in denser regions than late-type ones [17]. Environmental characteristics can be used in studying not only the formation and evolution of galaxies, but also their merging and interactions.

¹ VIPERS (VIMOS Public Extragalactic Redshift Survey), home page: <http://vipers.inaf.it>.



II. SAMPLE

VIPERS is the spectroscopic galaxy survey performed on VIMOS spectroscope at Very Large Telescope (VLT) [1, 2]. It covers the W1 and W4 regions of Canada–France–Hawaii Telescope Legacy Survey².

To follow the calculations and tests of the script, one has taken the whole VIPERS observe, which consists of W1 and W4 regions, having 18 and 11 subregions, respectively, in infrared filter i . Each subregion was divided into small images, or, the so called, poststamps, 100 by 100 pixels corresponding to 18.57 arcsec box size. To run the statmorph properly, it was necessary to filter accessed images with an appropriate script, the result of which reduced the initial number of objects. As a result, W1 part obtains 38742 galaxies and W4 — 27715. After discarding of images with instrumental issues, 58586 objects were gathered for morphological analysis. For the following research, based on the assumption about a dependence of Gini- M_{20} statistics on the redshift, we divided the whole data into 7 regions, related to different z from the lowest — 0.0016, to the highest — 1.2 (bigger redshifts were discarded). Details about the aforesaid division could be found in the Results sections.

III. METHOD

Within the current investigation, for the qualitative scrutiny of nonparametric approaches to studying the morphology of VIPERS galaxies and subsequent evaluation of statmorph’s capacity, Gini and M_{20} [7] parameters were used as major. Enunciation of the definition of those parameters in following subsections will contribute to the proper understanding of the resulting statistical diagrams.

Details of our method with illustrations are presented in the full version of the paper³.

A. The Gini coefficient

Gini(G) parameter is mainly used in economy theory for measuring the statistical dispersion intended to represent the income inequality or the wealth inequality within a nation or a social group [6]. For example, in a completely egalitarian society, Gini equals zero. In astronomy cases, for a set of n pixel flux values X_i , where $i = 1, 2, \dots, n$, the Gini coefficient can be computed as [18]:

$$G = \frac{1}{|\bar{X}|n(n-1)} \sum_{i=1}^n (2i - n - 1)|X_i|, \quad (1)$$

where $|\bar{X}|$ represents the mean over absolute values of X_i .

Gini coefficient takes a remarkably important part in the current investigation because it’s estimation is independent of the large-scale spatial distribution of the galaxy’s light. Also it can distinguish between galaxies with shallow light profiles and galaxies where much of the flux is located in a few pixels not at the projected center [7].

B. M_{20} coefficient

The total second-order moment M_{tot} is defined as a sum of fluxes in each pixel I_i multiplied by the squared distance to the galaxy center over all the pixels highlighted by the segmentation map [7]:

$$M_{\text{tot}} = \sum_{i=1}^n M_i = \sum_{i=1}^n I_i \cdot ((x_i - x_c)^2 - (y_i - y_c)^2), \quad (2)$$

where (x_c, y_c) are coordinates of the galaxy centre.

To remove the dependence of the morphology determination from the total galaxy flux or size the Gini coefficient is traditionally used in conjunction with the M_{20} , which is the essence of the second order moment of the brightest 20% of the galaxy’s flux [7]:

$$M_{20} \equiv \log_{10} \left(\frac{\sum_i M_i}{M_{\text{tot}}} \right), \quad \text{while } \sum_i I_i < 0.2 \cdot I_{\text{tot}}, \quad (3)$$

M_{20} plays an important role in tracing the spatial distribution of any bright nuclei, bars, spiral arms, and off-center star-clusters [7]. Moreover, it can be measured without circular or elliptical aperture approaches, and, furthermore, the center of the object galaxy is a free parameter.

C. Concentration

In 2000, a series of articles by Matthew Bershady and Christopher Conselice [8, 9, 12] introduced one of the modern systems of morphological parameters — the Concentration Asymmetry Smoothness or CAS system. Those papers argued that nowadays most galaxies at intermediate and high redshift are of an unusual, peculiar morphological type thus they can not be classified according to the traditional Hubble methods. From the system mentioned before, we have taken the Concentration parameter to analyze its dependence on Gini- M_{20} . It can be defined as:

$$C = 5 \log_{10} \frac{r_{80}}{r_{20}}, \quad (4)$$

where r_{20} and r_{80} are the radii of the circular aperture, which contain, respectively, 20 and 80 percent of the galaxy flux. This definition, according to the authors themselves, is stable enough to directly compare the concentration of galaxies at intermediate and high redshifts.

² CFHTLS(Canada–France–Hawaii Telescope Legacy Survey), home page: <https://www.cfht.hawaii.edu/Science/CFHLS/>.

³ <https://doi.org/10.13140/RG.2.2.24815.15523>, <https://arxiv.org/abs/2110.11666>

D. Bimodality test

To analyse images using the Statmorph code, we approximated PSF by two-dimensional Gaussian function with $\sigma = 2$ pixels. This number corresponds to $0.7''$, the mean value of FWHM of images in CFHTLS [1, 2].

We have performed two tests of morphological parameters for our sample. The aim of the first of them was to find a clear division of VIPERS galaxies into elliptical and spiral. This is important to test the method

of the Sersic index (n_s) calculation in the statmorph program. To find such bimodality, we have used $u-g$ color index from VIPERS database. Spiral galaxies must have $u-g < 1.3$ and $n_s > 0.7$. Elliptical galaxies must have $u-g > 1.3$ and $n_s < 0.7$. We used a sample of 4388 VIPERS galaxies from one W4 field $60' \times 60'$ centered at RA = 22h13m18s, DEC = +01d19m00s. For $0.2 < n_s < 10$ we have built (Fig. 1) a distribution of $u-g$ galaxy color versus the Sersic index and indicated four main regions with physically realistic values, which are quantitatively described in the Table 1 with other regions.

Region №	Region name	$u-g$ min	$u-g$ max	n_{\min}	n_{\max}	N
1	Very red	2	6	0	1095	22
2	Very blue	-6	0	0	1095	40
3	Weak	0	2	0.0004	0.001	184
4	Diffuse tail	0	2	0.001	0.35	169
5	Extreme	0	2	10	1095	284
6	Elliptical	1.3	2	0.7	10	356
7	Blue Elliptical	0	1.3	0.7	10	1132
8	Red spiral	1.3	2	0.45	0.7	253
9	Spiral	0	1.3	0.45	0.7	1446
10	Fake elliptical	1.3	2	0.35	0.45	85
11	Fake spiral	0	1.3	0.35	0.45	395

Table 1. Regions in the distribution of color index — Sersic index n for VIPERS galaxies shown in Fig. 1. N is the number of galaxies in the region

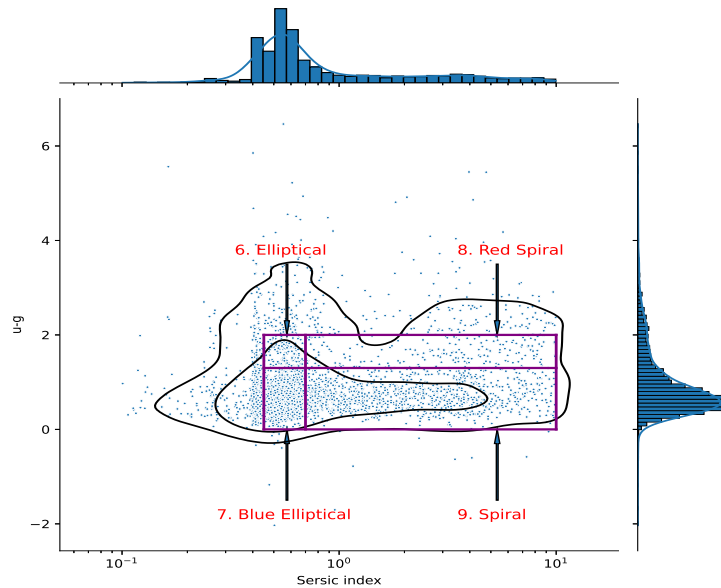


Fig. 1. The distribution of the $u-g$ galaxy color versus Sersic index. Marginal axes represent univariate histograms with the Gaussian kernel density estimations

Statmorph is affected by the artifacts from the algorithm of the Sersic index calculation. Affected parts of the distribution include ‘weak’ region N3 and ‘fake regions’ N10 and N11, described in Table 1. They originate from the lower bound of Sersic index in statmorph

and other special features of its calculation. We suppose that excluding both regions 10 and 11 we will still have enough galaxies and a correct proportion to detect the concentration of elliptical galaxies. The idea of the test was to compare a fraction of red galaxies for two ranges

of ns : 0.45–0.7 and 0.7–10. These fractions are equal to 15% and 24% respectively. This way, we have found that excess of elliptical galaxy number in region 6 is equal to 134 galaxies.

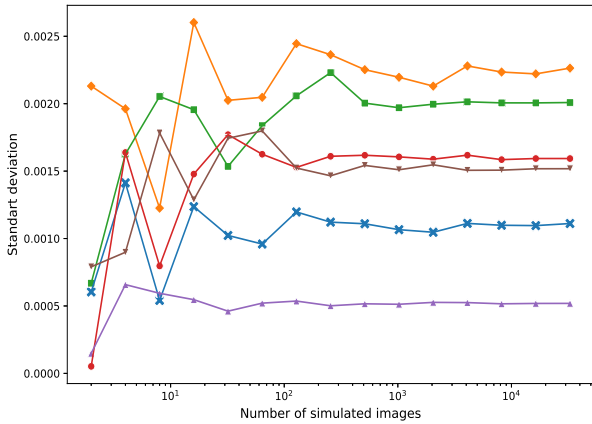


Fig. 2. Asymptotic limit of errors with an increase in the number of simulations. Errors of Gini are marked by crosses, M_{20} — diamonds, Concentration — squares, Asymmetry — triangles_up, Smoothness — circles, asymmetry rotated by 90 degrees — triangles_down

IV. ERROR ANALYSIS AND MERGER SIMULATION

Our error analysis of morphology parameters was performed on the basis of the statmorph tutorial ⁴. To evaluate errors of morphological parameters, we have simulated a set of different galaxy images with a random background. We considered values of the radii of simulated images from 0.6 to 4.5 arcsec. As a result, we have got exponential trends for increasing all parameter errors with infrared magnitude i and have fit them. In each fit we have used the values of magnitude from $i = 19$ to $i = 24$. The results of our simulations allow one to expect major problems with $i > 24$ and $r < 1$ arcsec. We also found asymptotic limits of errors of morphological parameters for a large number of simulated images Fig. 2.

As mentioned in previous sections, morphological parameters of galaxies are widely used in astrophysics. For example, they can be used for analysing galaxy mergers and interactions. We have performed simulations of images pairs without taking into account the physical interaction of galaxies and changes in their shape. These simulations were used to analyse the behavior of every morphological parameter from CAS/GM₂₀ statistics during a merging of two galaxies.

First of all, we have studied a variation of Gini and M_{20} parameters versus distance between merging galaxies. The change in Gini is the most inconspicuous, it

shifts between 0.4 to 0.5. The errors of defining this parameter are growing a lot at the distance of 15 pixels, but perceptibly decreasing at the distance of 20 pixels. M_{20} is changing a lot during the merge (between -1.6 to -1), although the resulting parameter remains constant.

For the variation in Smoothness and Asymmetry parameters, initial and final values (before and after the merge) remain constant, but the change in them is different. Smoothness has something like maximum near 10 pixels offset (peak from 13 to 6). It can be explained by dividing the starting segmentation map by two maps of two different galaxies. Asymmetry, at the same time, changes weakly (between 0 and 0.4).

The last one was the variation in Concentration analysis. Before merging (at 20 pixels distance), there was only one segmentation map, so the concentration was high. After decreased the distance, the segmentation map was divided into two regions, which significantly decreased the resulting concentration. But after merging, segmentation map had connected again, and concentration returned to its maximum.

Errors in all parameters were increasing during the division of the starting segmentation map at mid distances, and were decreasing during the connection of two maps into after merging at lower distances.

V. RESULTS

Using the information provided in the previous section, we have calculated the Gini coefficient and M_{20} for plotting the Gini (M_{20}) distribution, which is shown in the Fig. 3. The division into elliptical, spiral and merging galaxies is performed using the so called bulge statistics and merger statistics.

Bulge statistics indicates the morphological type of a galaxy. According to [13], it can be calculated by the following formula:

$$F = -0.693 \cdot M_{20} + 4.95 \cdot G - 3.96. \quad (5)$$

Merger statistics shows the distribution between regular and peculiar galaxies, for example, coalesced ones, and could be obtained as [13]:

$$S = 0.139 \cdot M_{20} + 0.99 \cdot G - 0.327. \quad (6)$$

The value $F = 0$ is the bound between spiral and elliptical galaxies. $F > 0$ corresponds to the elliptical galaxies and $F < 0$ refers to the spiral ones. Region $S > 0$ corresponds to merging or peculiar galaxies. One may see that the plotted distribution has a biased percentage of bimodality: E, S0 and Sa galaxies are much more rare than the spiral ones. This fact differs current investigation from the Rodriguez-Gomez one, in which the statmorph script was firstly used. As one may see, the bimodality in the mentioned work is more explicit, although the density contours does not confirm this statement. Potential discrepancies could be explained by

⁴ <https://nbviewer.jupyter.org/github/vrodgom/statmorph/blob/master/notebooks/tutorial.ipynb>

the difference between redshifts in the current paper and the compared one ($z \approx 0.05$ for the Pan-STARRS⁵ and 0.5–1.2 for VIPERS).

To validate the above assumption about the reasons for the discrepancy between the drawn graphs, the data was divided into several redshift ranges and investigated for its dependence on morphological parameters. The corresponding regions are distributed nearly normally

and have their maximum count at $z \approx 0.63$; the respective region, named “medium- z ”, consists of 22959 galaxies and lies between 0.6 and 0.8 z . The near-peak regions, called “Medium-low- z ” ($z = 0.4 - 0.6$) and “High- z ” ($z = 0.8 - 1.0$), contain 14852 and 13310, respectively. Objects from all remaining regions account for less than 13% of the data, so their contribution to the general pattern of the distribution is not significant.

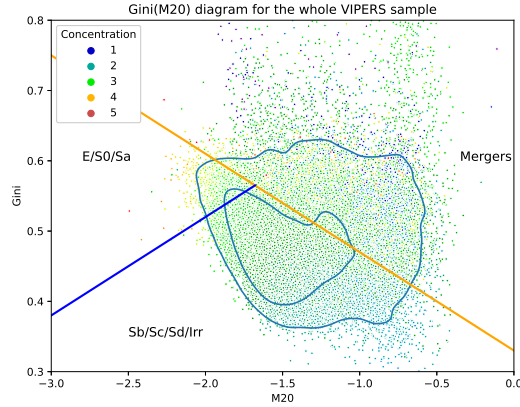


Fig. 3. Distribution of Gini versus M_{20} parameters. Bulge and merger statistics are shown as blue and orange lines, respectively. Colors of objects are based on a calculation of the Concentration parameter for each of them. Inner contour corresponds to 68% of the data sample around the most dense part of the distributions. Outer contour surrounds 95% of the data sample

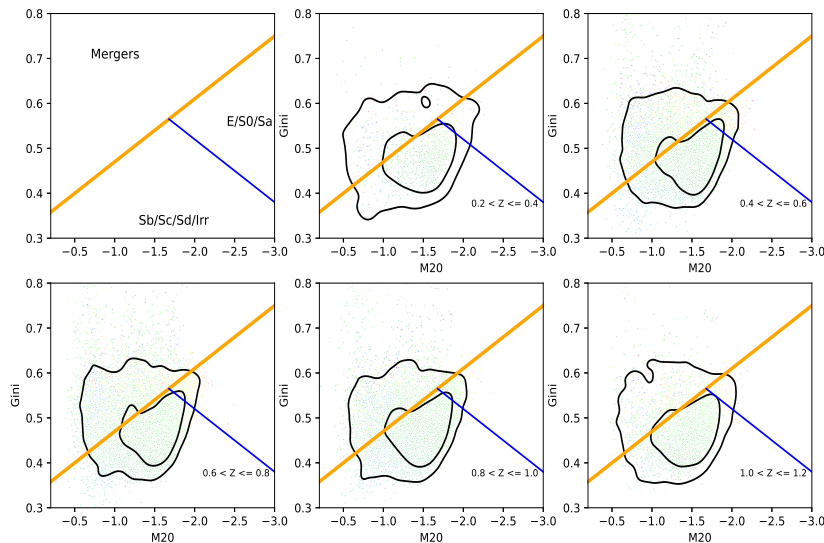


Fig. 4. Distributions of Gini versus M_{20} parameters for different redshifts from the lowest ($z > 0.2$) to the highest ($z \leq 1.2$). Contours are showing 68% and 95% of data. Colors of objects are based on a calculation of the Concentration parameter for each of them and are the same as they were for previous graph

For a qualitative analysis of the above mentioned assumption, already plotted distributions from the article by Jennifer Lotz [19] were used for comparison. In Fig. 4 one can see 5 graphs with the data structured

from the lowest to the highest redshifts with built density contours and bulge and merger statistics lines. The comparison between the plotted distributions and the graphs by Jennifer Lotz is reasonable because of similar z , but there are significant distinctions that affect the difference in the obtained results. First of all, one may notice that the percentage of late-type, or elliptical, galaxies in Lotz’s work prevails over the calculated percentage of the same objects but in VIPERS observe. It can be

⁵ Pan-STARRS — Panoramic Survey Telescope and Rapid Response System, home page: <https://panstarrs.stsci.edu/>

explained by the specifics of the data, which was used in the reference paper, as it was artificially cut in a large number of early type and peculiar galaxies, which are, eventually, dominating in the plotted distributions [19]. However, one could establish a similar nature in changing in the percentage of late and early type galaxies, if one paid attention to the contour, which corresponds to 68 percentage of the data sample. With a decreasing in the redshift, it slowly shifts towards elliptical galaxies. The exception is the group of small redshifts for which this contour motion falls out of the general trend. This difference may occur from the insufficiently high amount of galaxies of these redshifts. But, in general, the behavior of the sample objects described above coincides with generally accepted theories of the galactic evolution from spiral to elliptical due to coalescence or interactions.

VI. CONCLUSION

Gini- M_{20} statistics, as we know it nowadays, was first established in [7] where it was used to the built Gini- M_{20} distribution with the bulge statistics line. The main result of that work is the fact that almost all ‘normal’ galaxies from their data lie below that line. The same result can be notice of on our resulting graph, where a high amount of our data galaxies lies below the bulge statistics line, which immediately type them to late-type galaxies.

Bulge and merger statistics were applied in [19] to galaxies observed in All-wavelength Extended Groth Strip International Survey, AEGIS (Hubble Telescope) to find local merger candidates and to differ early and late-type galaxies at redshifts $0.2 < z < 1.2$. The authors mentioned the division between merger candidates and normal Hubble types. In this work, the also demonstrated the evidence for bimodality between early and late types.

The above mentioned Gini- M_{20} classification was used for merger diagnostics of simulated galaxies in [20]. In this paper, one may see the dependence of morphological parameters Gini- M_{20} and C on time, their in-time evolution. The main result, which is suggested in the paper, is that morphological evolution is not uniform.

Bulge statistics F based on Gini- M_{20} classification was analyzed in [21] for Illustris simulation. Besides the morphology classification, the following parameters were fitted with Bulge statistics: Star formation rate, stellar mass, galaxy size, and galaxy rotation.

All mentioned works demonstrate the same Gini- M_{20} distribution of different classes of galaxies as our work.

After the comparison of our Gini and M_{20} parameters with many other works, we confirm that our results are in agreement with the results, obtained by another authors.

Secondly, we have got satisfied statistical errors for the results presented in our paper. Some disagreement between our and other above mentioned papers are within statistical errors ranges.

The results, which are shown in this paper, could be used in further studies of the influence of merging and environment on the galaxy morphology, and for advanced classification of galaxies on the basis of their morphological parameters via the statmorph code.

Acknowledgement.

This work has been supported by the Ministry of Education and Science of Ukraine: Grant of the Ministry of Education and Science of Ukraine for perspective development of a scientific direction “Mathematical sciences and natural sciences” at Taras Shevchenko National University of Kyiv. This research was done with the support of the Center for the Collective Use of Scientific Equipment “Laboratory of high energy physics and astrophysics”. The work of L. V. Zadorozhna was supported by the grant No. UMO-2018/30/Q/ST9/00795 from the National Science Centre, Poland.

-
- [1] L. Guzzo *et al.*, *Astron. Astrophys.* **566**, 21 (2014); <https://doi.org/10.1051/0004-6361/201321489>.
 - [2] M. Scodreggio *et al.*, *Astron. Astrophys.* **609**, 14 (2018); <https://doi.org/10.1051/0004-6361/201630114>.
 - [3] N. Malavasi *et al.*, *Mon. Not. R. Astron. Soc.* **465**, 3817 (2017); <https://doi.org/10.1093/mnras/stw2864>.
 - [4] J. Krywult *et al.*, *Astron. Astrophys.* **598**, 18 (2017); <https://doi.org/10.1051/0004-6361/201628953>.
 - [5] J. L. Sérsic, *Boletín de la Asociación Argentina de Astronomía* **6**, 41 (1963).
 - [6] C. Gini, *Variabilità e mutabilità: contributo allo studio delle distribuzioni e delle relazioni statistiche* (Tipografia di Paolo Cuppini, Bologna, 1912).
 - [7] J. M. Lotz, J. Primack, P. Madau, *Astron. J.* **128**, 163 (2004); <https://doi.org/10.1086/421849>.
 - [8] M. A. Bershadly, A. Jangren, C. J. Conselice, *Astron. J.* **119**, 2645 (2000); <https://doi.org/10.1086/301386>.
 - [9] C. J. Conselice, *Astrophys. J. Suppl. Ser.* **147**, 1 (2003); <https://doi.org/10.1086/375001>.
 - [10] D. Schade *et al.*, *Astrophys. J. Lett.*, **451**, 1 (1995); <https://doi.org/10.1086/309677>.
 - [11] R. G. Abraham *et al.*, *Mon. Not. R. Astron. Soc.* **279**, L47 (1996); <https://doi.org/10.1093/mnras/279.3.L47>.
 - [12] C. J. Conselice, M. A. Bershadly, A. Jangren, *Astrophys. J.* **529**, 886 (2000); <https://doi.org/10.1086/308300>.
 - [13] V. Rodriguez-Gomez *et al.*, *Mon. Not. R. Astron. Soc.* **483**, 4140 (2019); <https://doi.org/10.1093/mnras/sty3345>.
 - [14] L. de Ravel *et al.*, *Astron. Astrophys.* **498**, 22 (2009); <https://doi.org/10.1051/0004-6361/200810569>.
 - [15] P. Kampczyk *et al.*, *Astrophys. J.* **762**, 38 (2013); <https://doi.org/10.1088/0004-637X/762/1/43>.
 - [16] L. A. M. Tasca *et al.*, *Astron. Astrophys.* **503**,

- 379 (2009); <https://doi.org/10.1051/0004-6361/200912213>.
- [17] A. Oemler, Jr., *Astrophys. J.* **194**, 1 (1974); <https://doi.org/10.1086/153216>.
- [18] G. J. Glasser, *J. Am. Stat. Assoc.* **57**, 648 (1962); <https://doi.org/10.1080/01621459.1962.10500553>.
- [19] J. M. Lotz *et al.*, *Astrophys. J.* **672**, 177 (2008); <https://doi.org/10.1086/523659>.
- [20] G. F. Snyder *et al.*, *Mon. Not. R. Astron. Soc.* **451**, 4290 (2015); <https://doi.org/10.1093/mnras/stv1231>.
- [21] G. F. Snyder *et al.*, *Mon. Not. R. Astron. Soc.* **454**, 1886 (2015); <https://doi.org/10.1093/mnras/stv2078>.

РОЗШИРЕНА МОРФОЛОГІЯ ГАЛАКТИК VIPERS

О. Гугнін¹, А. Тугай¹, Н. Пулатова^{2,3}, Л. Задорожна^{1,4}

¹Київський національний університет імені Тараса Шевченка, вул. Глушкова, 4, Київ, 03127, Україна,

²Головна астрономічна обсерваторія Національної академії наук України,
вул. Академіка Заболотного, 27, Київ, 03143, Україна,

³Інститут астрономії Макса Планка, Гайдельберг, Німеччина,

⁴Факультет фізики, астрономії та прикладної інформатики, Ягеллонський університет, Краків, Польща

Ми розрахували морфологічні параметри для тестового зразка в 4659 галактиках з огляду VIPERS (спектроскопічний огляд галактик, проведений на спектроскопі VIMOS на VLT). Ці параметри включають $Gini$, M_{20} , концентрацію, асиметрію та гладкість. Результати корелюють із розподілом цих параметрів для інших модельованих та спостережуваних вибірок. Ми також дослідили залежність цих параметрів від індексу Серсіка радіального розподілу поверхневого блиску зображення галактики. Нашою метою було чітке розділення галактик VIPERS на еліптичні та спіральні, необхідне для перевірки методу розрахунку індексу Серсіка (ns) у програмі *statmorph*. Щоб знайти таку бімодальність, ми використовували індекс кольору $B-V$ з бази даних VIPERS.

Для аналізу похибок морфологічних параметрів ми змодельовали зображення галактик із випадковим фоном різної величини та оцінили похибки як дисперсію цих параметрів. Ми також знайшли асимптотичні значення похибок морфологічних параметрів, збільшуючи кількість симульованих зображень.

Наступним етапом роботи була симуляція пар зображень задля того, щоб проаналізувати можливі зміни кожного морфологічного параметра під час накладання зображень близьких галактик. У результаті цього дослідження ми проаналізували залежність кожного морфологічного параметра зі статистики CAS та $Gini-M_{20}$ від відстані між центрами галактик.

Відмінності між нашими результатами щодо розподілу $Gini-M_{20}$ для галактик VIPERS та PanStarrs при $z < 0.5$ можна пояснити космологічною еволюцією галактик. Ми з'ясували, що в сучасному Всесвіті еліптичних галактик набагато більше, ніж за $z > 0.5$, що відповідає вибірці VIPERS. Також ми дійшли висновку, що злиття галактик у ранньому Всесвіті відбувалося частіше.

Ключові слова: Галактики: фотометрія, космологія: великомасштабна структура Всесвіту.